Received 8 December 2022; revised 29 December 2022; accepted 9 January 2023. Date of publication 12 January 2023; date of current version 25 January 2023.

Digital Object Identifier 10.1109/OJCOMS.2023.3236319

Ensemble Learning-Based Edge Caching Strategies for Internet of Vehicles: Outage and Finite SNR Analysis

TAN ZHENG HUI ERNEST [1] AND A. S. MADHUKUMAR [2] (Senior Member, IEEE)

[1] Advanced Remanufacturing and Technology Centre, Agency for Science, Technology and Research, Singapore

[2] School of Computer Science and Engineering, Nanyang Technological University, Singapore

CORRESPONDING AUTHOR: T. Z. H. ERNEST (e-mail: ernest_tan@artc.a-star.edu.sg)

This work was supported by the Agency for Science, Technology and Research (A*STAR), Singapore.

ABSTRACT In this paper, an ensemble learning-driven edge caching (ELDEC) strategy and a meta-based ensemble learning-driven edge caching (MELDEC) strategy are proposed for content popularity prediction and cache content placement in Internet-of-Vehicles (IoV) networks. Specifically, the proposed MELDEC and ELDEC strategies incorporate meta learning and ensemble learning for enhanced content popularity prediction in IoV networks. Closed-form outage probability and finite signal-to-noise ratio (SNR) diversity gain expressions are also derived to establish the relationship between the proposed edge caching strategies and the wireless performance of IoV networks. When compared against benchmark schemes, the proposed MELDEC and ELDEC strategies achieve near-optimal cache hit rates, outage probability, and finite SNR diversity gain under imperfect channel state information (CSI) estimation. We also show that the outage probability decay rate in the IoV network depends on the number of base stations and roadside units, and it is independent of the content popularity prediction of the MELDEC strategy, ELDEC strategy, and benchmark schemes. The performance analysis demonstrates that the proposed MELDEC and ELDEC strategies are promising solutions towards achieving reliable content access in IoV networks.

INDEX TERMS Deep learning, ensemble learning, meta learning, multi-access edge computing, edge caching, Internet-of-Vehicles, vehicular networks, outage probability, finite signal-to-noise ratio (SNR), diversity.

I. INTRODUCTION

RECENT interests to support connected vehicles (CVs), road side units (RSUs), and cellular base stations (BSs), as part of next-generation intelligent transportation systems (ITSs) have necessitated a transition towards Internet-of-Vehicles (IoV) networks [1], [2], [3]. Such IoV networks are envisioned to be able to meet the mission-critical requirements of ITS applications. However, one challenge in realizing IoV networks lies in the fact that the intensity of information exchanged in ITS applications ultimately results in significant backhaul overheads [4]. Apart from backhaul overheads, developing frameworks for accurate outage and finite signal-to-noise (SNR) characterization and identification of performance bounds in IoV networks remain an open research problem due to vehicular mobility, wireless channel environment, and the accurate modeling of RSU and BS placements for vehicular communications [5].

To reduce backhaul overheads, one can turn towards the concept of edge caching from the multi-access edge computing (MEC) paradigm [6], [7], [8]. The main idea is to employ edge caching in IoV networks to reduce overall backhaul overheads by proactively storing, i.e., caching, popular contents at MEC servers located near CVs [4], e.g., cellular BSs or RSUs. In this aspect, the adoption of edge caching in IoV networks has been widely studied in the literature, e.g., [4], [5], with studies investigating the application of deep learning for edge caching and the performance of edge caching in IoV networks.

A. RELATED WORKS

1) DEEP LEARNING-BASED EDGE CACHING IN IOV NETWORKS

In the literature, studies employing deep learning-driven schemes for content popularity prediction and placement in edge caching have been noted in IoV networks. For example, the authors in [9] proposed an edge caching scheme based on cross-entropy to determine popular contents that should be cached at RSUs. An analysis showed that the proposed edge caching scheme achieves higher cache hit rates and lower latency than other benchmark non-learning schemes. In [10], deep reinforcement learning and particle swarm schemes are employed as part of an edge caching and resource allocation framework in IoV networks. Likewise, the authors in [11] propose a cooperative deep reinforcement learning-based edge caching scheme, while [12] proposed a convolutional neural network-based edge caching scheme to predict the popularity of infotainment contents.

It is evident from [9], [10], [11], [12] that the focus has largely been on enhancing the content popularity prediction accuracy. Yet, the proposed schemes can be computationally complex to implement in practice. In turn, this may lead to longer execution time and unnecessary backhaul overheads. Furthermore, the performance characterization of deep learning-based edge caching schemes to identify performance bounds in IoV networks remains unaddressed.

2) PERFORMANCE CHARACTERIZATION OF CACHE-ENABLED IOV NETWORKS

As noted earlier, the performance of cache-enabled wireless networks has been widely investigated in the literature. In [13], [14], the successful content delivery probability was analyzed for different cooperative schemes in cellular networks where closed-form expressions for coverage probability were provided and evaluated to identify performance bounds. Likewise, the content retrieval delay in cooperative cellular networks was analyzed in [15] while [16] characterized the successful content delivery performance for backhaul-limited cache-enabled heterogeneous networks. In [17], the successful content delivery probability was analyzed for reinforcement learning-based probabilistic caching with a priori knowledge of content popularity. Similar successful content delivery probability analysis was also conducted in [18] for online content popularity prediction techniques. In [19], an outage probability analysis was also noted for deep learning-based edge caching in device-to-device networks.

For IoV networks, the outage probability and content retrieval delay for in-vehicle caching was investigated in [20]. Similar studies on coverage probability analysis have also been noted in [4] and [5]. Apart from outage and coverage probability, finite SNR analysis is another useful tool to aid in the performance characterization of wireless networks. In particular, finite SNR analysis enables one to evaluate the finite SNR diversity gain of wireless networks [21], [22], [23], [24]. The finite SNR diversity gain of wireless networks effectively quantifies the outage probability decay rate for a given SNR [23]. With finite SNR analysis, one can uncover outage probability behaviors which are noticeable at only finite SNR regimes, e.g., SNRs below 30dBm. As most wireless networks operate at finite SNR regimes [24], finite SNR analysis has been shown to be useful in providing accurate outage probability characterizations. For instance, finite SNR diversity gain has been employed in unmanned aerial vehicle networks to determine interference-limited scenarios [21], [24].

Yet, there remains limited studies on employing finite SNR analysis for performance characterization in IoV networks. In addition, the above mentioned studies, i.e., [4], [5], [13], [14], [15], [16], [17], [20], have assumed a priori knowledge of content popularity while the study in [18] assumed that all future content popularity predictions are related to past predictions. However, content popularity knowledge in edge caching-based wireless networks is unavailable in practice [18], may be unrelated to past content popularity knowledge, and that assuming otherwise may lead to an unrealistic outage and finite SNR characterization. Furthermore, the performance analysis insights in [13], [14], [15], [16], [17], [18], [19] have limited applications outside of IoV networks.

B. MAIN MOTIVATIONS AND CONTRIBUTIONS

To address the above challenges, we propose an ensemble learning-driven edge caching (ELDEC) strategy that incorporates ensemble learning and a meta-based ensemble learning-driven edge caching (MELDEC) strategy which combines both meta and ensemble learning for edge caching in IoV networks.

Ensemble learning allows for the outputs of weaker learning models to be combined to enhance prediction performance [25], [26], while meta learning enables one to optimally combine the outputs of several weaker learning models [26]. By leveraging on meta and ensemble learning, simple deep learning models can be used for content popularity prediction in IoV networks. Specifically for the MELDEC strategy, meta learning is employed to optimally prioritize better performing deep learning models within an ensemble of base deep learning models for enhanced content popularity prediction. It is also worth noting that the amalgamation of meta learning with ensemble learning has not been widely investigated for content popularity prediction in edge caching. This is in contrast to the techniques noted in [9], [10], [11], [12], which have focused on enhancing content popularity prediction at the expense of potentially higher computational complexity.

A comprehensive outage and finite SNR analysis framework is also presented for the performance characterization of the MELDEC strategy, ELDEC strategy, and considered benchmark schemes in the IoV network. Specifically, outage probability and finite SNR diversity gain expressions are obtained in closed-form for the MELDEC strategy, ELDEC strategy, and benchmark schemes by extending the

power series approaches proposed in [21] and [27] for IoV networks. The power series approach enables complicated functions to be expressed as a power series, leading to a rigorous analysis of the interplay between CV mobility, stochastic geometry, outage probability, and finite SNR diversity gain. To the best of our knowledge, such a performance characterization framework for deep learning-based edge caching schemes in IoV networks is unavailable in the literature.

Therefore, the main contributions of this paper are summarized as follows:

- This paper proposes MELDEC and ELDEC for content popularity prediction and cache content placement in IoV networks, which to the best of our knowledge, has not been investigated in the literature.
- Closed-form outage probability and finite SNR diversity gain expressions are derived for the proposed MELDEC strategy, ELDEC strategy, and benchmark schemes to characterize and identify performance bounds in the IoV network.
- We demonstrate that the proposed MELDEC and ELDEC strategies achieve near-optimal cache hit rates, outage probability, and finite SNR diversity gain when compared against the benchmark deep learning-based technique in [28] and non-learning based benchmark schemes under imperfect channel state information (CSI) estimation.
- When ideal CSI estimation is attained, we demonstrate through finite SNR analysis that the content popularity prediction accuracy of the MELDEC strategy, ELDEC strategy, and benchmark schemes plays a limited role in the overall outage probability decay. Instead, the outage probability decay is greatly influenced by the number of cellular BSs and RSUs, and the severity of small-scale fading in the IoV network.

The remainder of this paper is organized as follows. The proposed system model is introduced in Section II, with the MELDEC and ELDEC strategies presented in Section III. The closed-form outage probability and energy efficiency expressions are derived Section IV. Finally, the results of the numerical analysis are presented in Section IV, with the conclusions and future research directions of the paper discussed in Section VI. A summary of key mathematical notations used in this paper is also provided in Table 1.

TABLE 1. Summary of key mathematical notations.

Notations	Description
$\bar{P}_t$; P_t	Normalized transmit power; Transmit Power
r_a	Communication radius
h_x	Channel gain of node-x
$\hat{h}_x$	Estimated channel gain of node-x
e_x	CSI estimation error for node-x
v; ϵ	Vehicle speed (m/s); Correlation coefficient
L_0; η	Pathloss; Noise power (dBm)
m_x	Nakagami-m fading parameter for $\lvert\hat{h}_x\rvert^2$
μ_x	Nakagami-m fading parameter for $\lvert e_x\rvert^2$
M_{RSU}; M_{BS}	Number of RSUs; Number of cellular BSs
K_{total}; K_{size}	Total number of files; File size
K_{cache}	RSU cache size
f_k	Request probability of the k-th file
K_{model}	Number of deep learning models for ELDEC
$K_{\text{model,meta}}$	Number of deep learning models for MELDEC
$\mathbf{X}$; M_{dataset}	Content demand table; Number of rows in $\mathbf{X}$
$\mathbf{X}_m$; $\mathbf{y}_m$	m-th sample in $\mathbf{X}$; Ground truth
M_{train}	Number of training samples
M_{test}	Number of testing samples
$\hat{\mathbf{f}}$	Vector for content popularity prediction
$\hat{\mathbf{f}}_{\text{cache}}$	Vector containing index of files to be cached
$\bar{\mathbf{y}}_{s,\nu,k}$	Cache content score of file-k for the s-th test sample that is predicted with the ν-th deep learning model
$P_{\text{hit},u}$	Estimated cache hit rate
P^u_{out}	Outage probability of the CV
$P^u_{\text{out,Ideal CSI}}$	Outage probability of the CV under ideal CSI
d^u_f	Finite SNR diversity gain of the CV
$d^u_{f,\text{Ideal CSI}}$	Finite SNR diversity gain of the CV under ideal CSI

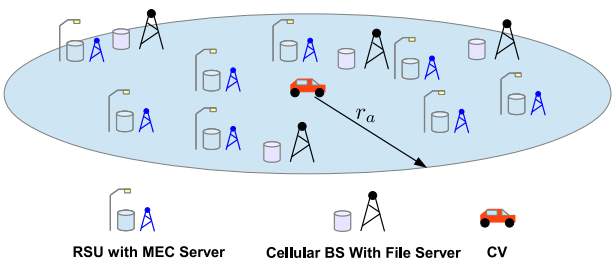

FIGURE 1. A CV in an IoV network communicating with RSUs and cellular BSs.

II. SYSTEM MODEL

In this work, we consider an IoV network comprising M_{RSU} RSUs and M_{BS} cellular BSs (Fig. 1). Specifically, we are interested in analyzing downlink cellular transmissions between the typical CV and the infrastructure when edge caching is adopted in the IoV network.[1] As part of the analysis, we assume that downlink cellular transmissions are impaired by imperfect CSI due to Doppler shift from the mobility of CVs [29], [30] and small-scale fading effects [31], [32]. Furthermore, network coordination within the IoV network is assumed to occur either among RSUs or BSs through horizontal handovers, or between RSUs and BSs through vertical handovers [33].

A. STOCHASTIC GEOMETRY MODEL

To model the spatial locations of the RSUs and cellular BSs, the binomial point process (BPP) model is employed in this study. The BPP model is used to model the uniform distribution of distances in a finite-sized cell for a fixed number of nodes [34], [35]. In the context of IoV networks, the number of RSUs, cellular BSs and CVs operating in a geographical area is generally known in practice. Therefore, the BPP model is more suitable than Poisson point processes

1. Enhancing the performance of the IoV network through cache-enabled vehicle-to-vehicle links is being investigated as an extensions of this work.

(PPPs) to model the distance distribution of nodes in an IoV network.

Let the typical CV associated to the RSUs or cellular BSs be at the origin $\mathcal{O}$ with a communication radius of r_a. Then, the spatial location of the RSUs and cellular BSs are assumed to be uniformly distributed in a disc centered at the CV with radius r_a and angle $[0, 2\pi)$. The Euclidean distance between BS-i and the CV is denoted as d_i, while the Euclidean distance between RSU-j and the CV is denoted as d_j. From [34, eq. (3)], [27], the probability density function (PDF) $f_{d_x}(w)$ of $d_x, x \in \{i, j\}$ is given as $f_{d_x}(w) = \frac{2w}{r_a^2}$ where $0 \leq w \leq r_a$.

B. MOBILITY MODEL

In the IoV network, the CV is associated with the cellular BS or the RSU with the strongest instantaneous signal-to-interference-plus-noise ratio (SINR) and CSI is estimated at the CV over a feedback period T [29], [30]. We denote $h_x, x \in \{i, j\}$ as the channel gain between node-x and the CV, $\hat{h}_x$ as the estimated channel gain, e_x as the CSI estimation error, and $0 < \epsilon < 1$ as the correlation coefficient between h_x and h_{x+1}. Using Jakes' statistical model, ϵ is defined as [29], [30], [36], [37]:

$$\epsilon = J_0(2\pi f_d T), \tag{1}$$

where J_0 is the zero-order Bessel function of the first kind [38, eq. (9.1.10)], $f_d = \frac{v f_c}{c}$ is the maximum Doppler frequency, f_c is the carrier frequency, v is the vehicle speed in m/s, and $c = 3 \times 10^8$ m/s. Then, we employ the first-order Gauss-Markov process to model h_x such that $h_x = \epsilon \hat{h}_x + \sqrt{1 - \epsilon^2} e_x$ [29], [30], [36], [37].

C. CHANNEL MODEL AND INSTANTANEOUS SINR

At the CV, the instantaneous SINR of cellular transmissions from BS-i (γ_i) or RSU-j (γ_j) is given as [29]:

$$\gamma_x = \frac{\left|\hat{h}_x\right|^2 d_x^{-l}}{1 + |e_x|^2 d_x^{-l}}, \tag{2}$$

where l is the pathloss exponent and $x \in \{i, j\}$.

We assume $|\hat{h}_x|^2$ follows the Gamma distribution with average received power $\bar{P}_t \epsilon^2$ and Nakagami-m fading parameter $m_x, x \in \{i, j\}$, i.e., $|\hat{h}_x|^2 \sim \text{Nak}(\bar{P}_t \epsilon^2, m_x)$, where $\bar{P}_t = \frac{P_t}{L_0 \eta}$ is the normalised transmit power, P_t is the transmit power, L_0 is the pathloss at 1 m reference distance [39], $\eta = -174 + 10 \log_{10}(B_\text{w})$ is the noise power in dBm, and B_w is the bandwidth. Likewise, we assume $|e_x|^2 \sim \text{Nak}(\bar{P}_t(1 - \epsilon^2), \mu_x), x \in \{i, j\}$. Such an approach allows a multitude of small-scale fading effects to be modeled for both $|\hat{h}_x|^2$ and $|e_x|^2$, e.g., Rayleigh fading [29], [30].

D. FILE POPULARITY MODEL

A finite library of K_total files is assumed in the IoV network, where each file has a size of K_size. CVs in the IoV network transmit file requests to both RSUs and cellular BSs such that the file requests are first transmitted to the RSUs, and if the requested file is unavailable at the RSU, then the file request is serviced by cellular BSs.

To model file popularity and placement in the IoV network, we assume that RSUs are equipped with MEC servers that have a cache size of K_cache, and cellular BSs are equipped with file servers hosting the library of K_total files such that $1 \leq K_\text{cache} \leq K_\text{total}$ [19]. Furthermore, it is assumed that *the popularity of each file is unknown* since file request patterns are dynamically changing in practice. However, for the sake of analysis, the popularity of the k-th file is assumed to follow a Zipf distribution and the request probability of file-k, $1 \leq k \leq K_\text{total}$ is given as $f_k = \frac{k^{-z}}{\sum_{j=1}^{K_\text{total}} j^{-z}}$, where z is the file popularity factor [13].

As the popularity of each file is unknown, the main aim of this paper is to propose an ELDEC strategy for IoV networks to enable file popularity prediction and caching at RSUs.

III. ENSEMBLE LEARNING-BASED EDGE CACHING STRATEGIES

In this section, detailed descriptions pertaining to the proposed ELDEC strategy, MELDEC strategy, and benchmark schemes are provided.

A. PROPOSED ELDEC STRATEGY

The proposed ELDEC strategy incorporates ensemble learning to predict the popularity of all K_total files based on file request statistics from CVs in the IoV network. In ensemble learning, multiple base learning models are trained and the resultant outputs are amalgamated for improved prediction accuracy, e.g., [26]. On its own, such base learning models may produce lower prediction accuracy. However, if orchestrated properly, a set of base learning models can be applied to achieve greater prediction or classification accuracy [25]. One tradeoff to such an approach is the need to train additional base learning models, which can be computationally intensive and may lead to longer training time. However, in the context of IoV networks, this can be mitigated by distributing the training of base learning models across an IoV network to RSUs and cellular BSs with sufficient processing capability.

Therefore, we apply ensemble learning for edge caching by training an ensemble of K_model deep learning neural network (DNN) models using the file request statistics. Thereafter, the prediction output from each DNN model is combined into a single prediction output for all K_total files. Files with high predicted popularity are then cached at RSUs to improve the overall performance of the IoV network. Such a technique has also been adopted in similar studies, e.g., [26], [28].

1) DATASET GENERATION

In the IoV network, all file indices requested by CVs are tracked by RSUs and are periodically uploaded for content

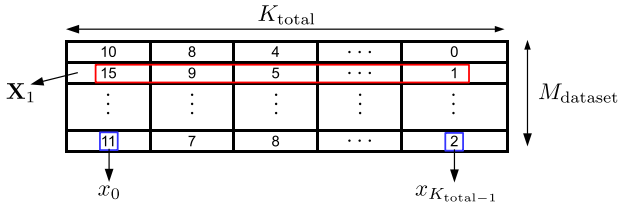

FIGURE 2. An illustration of the content demand table (X).

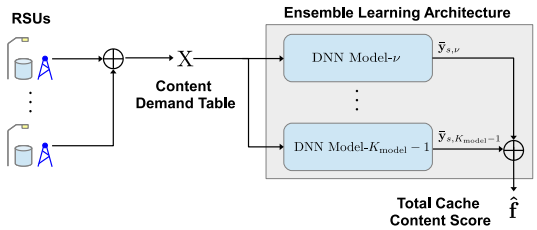

FIGURE 3. An illustration of the proposed ELDEC strategy with ensemble learning.

popularity prediction over a wired backhaul link to a cloud-based deep learning platform.[2] The deep learning platform maintains a content demand table ($\mathbf{X}$) with M_{dataset} rows by aggregating all file indices which have been requested by CVs at each RSU. For the m-th row ($\mathbf{X}_m$), i.e., the m-th sample or m-th row in $\mathbf{X}$, the deep learning platform tabulates the vector $\mathbf{X}_m = [x_0, \ldots, x_k, \ldots, x_{K_{\text{total}}-1}]$ from all RSUs to obtain the instantaneous file access pattern across the IoV network, where x_k denotes the total number of times file-k was requested, before $\mathbf{y}_m = \mathbf{X}_m$ is obtained as the ground truth label of $\mathbf{X}_m$ (Fig. 2).[3,4] After populating $\mathbf{X}$, M_{train} training samples and M_{test} testing samples are randomly selected from $\mathbf{X}$ for training and testing such that $\mathbf{X}_m$ is used as the input to each DNN model. The objective behind such an arrangement is to predict the cache content score of file-k for content popularity prediction, where $0 \leq k \leq K_{\text{total}} - 1$.

2) ENSEMBLE ARCHITECTURE

An ensemble of K_{model} DNN models are trained with the main goal of predicting the total cache content score for each file (Fig. 3). Together, the K_{model} DNN models make up an ensemble architecture and each DNN model comprises an input layer, hidden layers, and an output layer. We employ fully connected layers in the DNN model, with a rectified linear unit, i.e., ReLU, used as the activation function for some of the hidden layers.

2. Examples of such platforms include Microsoft Azure and Google Compute Engine.

3. It is worth noting that the DNN models used in this work only require file index information for content popularity prediction. Future works will investigate utilizing additional information, e.g., SINR, CV mobility and, content lifespan [40], together with distributed learning-based or cooperative-based methods, e.g., [28], [41], [42] to enhance the accuracy of content popularity prediction.

4. In other words, $\mathbf{X}_m$ indicates the total number of requests for file-k in the IoV network, which is obtained from all RSUs.

TABLE 2. DNN model design.

Layer	Output Dimensions
Input	$1 \times K_{\text{total}}$
Flatten	K_{total}
Dense + ReLU	128
Dense + ReLU	128
Dropout	128
Dense	K_{total}
Softmax	K_{total}

Using the training and testing samples, each DNN model is trained to minimize the categorical cross-entropy loss function. Finally, softmax [43] is used as the activation function for the output layer and the Adam optimiser is employed for weight update. A description of the DNN model design is provided in Table 2, where a dropout fraction rate of 0.1 is used.

3) OFFLINE TRAINING AND DEPLOYMENT

The K_{model} DNN models in the ELDEC strategy are trained offline and validated online using the cloud-based deep learning platform with M_{train} samples and M_{test} samples, respectively. Specifically, the vector $\hat{\mathbf{f}}$ is obtained during online validation using M_{test} test samples for content popularity prediction. Starting with the s-th test sample for the ν-th DNN model, an output vector $\bar{\mathbf{y}}_{s,\nu} = [\bar{\mathbf{y}}_{s,\nu,0}, \ldots, \bar{\mathbf{y}}_{s,\nu,K_{\text{total}}-1}]$ with K_{total} elements is obtained, where $\bar{\mathbf{y}}_{s,\nu,k}$ is the cache content score of file-k for the s-th test sample that is predicted with the ν-th DNN model.[5] Then, the vector $\hat{\mathbf{f}}$ is obtained as:

$$\hat{\mathbf{f}} = \left[\left(\sum_{\nu=0}^{K_{\text{model}}-1} \sum_{s=0}^{M_{\text{test}}-1} \bar{\mathbf{y}}_{s,\nu,0} \right), \ldots, \left(\sum_{\nu=0}^{K_{\text{model}}-1} \sum_{s=0}^{M_{\text{test}}-1} \bar{\mathbf{y}}_{s,\nu,K_{\text{total}}-1} \right) \right], \tag{3}$$

where $\sum_{\nu=0}^{K_{\text{model}}-1} \sum_{s=0}^{M_{\text{test}}-1} \bar{\mathbf{y}}_{s,\nu,k}$ is the total cache content score of file-k.

The vector $\hat{\mathbf{f}}$ is used to determine the total cache content score of each file based on the ensemble learning of the K_{model} DNN models. As files with larger cache content scores are more likely to be requested, the top K_{cache} files with the highest cache content scores in $\hat{\mathbf{f}}$ are cached at RSUs, with the corresponding file index populated in a vector $\hat{\mathbf{f}}_{\text{cache}}$. A summary of the offline training and deployment process for the ELDEC strategy is presented in Algorithm 1 and illustrated in Fig. 3.

4) ESTIMATED CACHE HIT RATE

Based on $\hat{\mathbf{f}}_{\text{cache}}$, the estimated cache hit rate of the ELDEC strategy $P_{\text{hit,EL}}$ is obtained as [44], [45]:

$$P_{\text{hit,EL}} = \frac{\sum_{s=0}^{M_{\text{test}}-1} \mathbf{1}(s)}{\sum_{s=0}^{M_{\text{test}}-1} \sum_{k=0}^{K_{\text{total}}} x_k}, \tag{4}$$

5. It is important to note that since M_{test} testing samples are randomly selected from $\mathbf{X}$, the s-th test sample is also a vector which is tabulated as $[x_0, \ldots, x_k, \ldots, x_{K_{\text{total}}-1}]$.

Algorithm 1 ELDEC Offline Training and Deployment

Input: $\mathbf{X}$, K_{model}, M_{test}, M_{train}, K_{total}
Output: $\hat{\mathbf{f}}_{\text{cache}}$

```
Randomly select M_train samples from X for training.
Allocate remaining M_test samples from X for validation.
for ν = 0, 1, ..., K_model − 1 do
    Build DNN model-ν using Table 2.
    Train DNN model-ν with M_train samples.
    for s = 0, 1, ..., M_test − 1 do
        for k = 0, 1, ..., K_total − 1 do
            Compute ȳ_{s,ν,k}.
        end for
        Compute ȳ_{s,ν}.
    end for
end for
Compute f̂ and f̂_cache.
Populate all RSUs with files indicated in f̂_cache.
```

where the total number of requests in the M_{test} testing samples is computed in the denominator of (4), and $\mathbf{1}(s) = x_k$ if the k-th file requested in the s-th sample is in $\hat{\mathbf{f}}_{\text{cache}}$.

After calculating $P_{\text{hit,EL}}$ and caching the K_{cache} files at RSUs, the content demand table ($\mathbf{X}$) is emptied and repopulated with new file index information aggregated from all RSUs until M_{dataset} samples are collected.[6] Offline training and content popularity prediction are then conducted with the ensemble of K_{model} DNN models, and $P_{\text{hit,EL}}$ recalculated, before the updated K_{cache} files are cached at RSUs. In this way, the ELDEC strategy continues to predict popular contents which are relevant in the near future even under time-varying content request statistics.[7]

B. PROPOSED MELDEC STRATEGY

It is worth noting that the ELDEC strategy considers all DNN models equally when computing the predicted total cache content score of each file, i.e., $\hat{\mathbf{f}}$. Therefore, we propose the MELDEC strategy that incorporates meta learning and ensemble learning to further improve content popularity prediction accuracy. The main idea behind the MELDEC strategy is to employ a meta model within a meta-based ensemble learning architecture to aid in prioritizing better performing learners from within an ensemble of base learners such that $\hat{\mathbf{f}}$ more accurately reflects actual content popularity.

1) META-BASED ENSEMBLE LEARNING ARCHITECTURE

An ensemble of $K_{\text{model,meta}}$ DNN models are trained for content popularity prediction using the design described in Table 2. The output from each of the $K_{\text{model,meta}}$ DNN models are then aggregated as inputs into a meta model which comprises an input layer, hidden layers, and an output layer. The meta model employs fully connected layers, with ReLU used in the hidden layers. The resulting meta-based ensemble learning architecture comprises $K_{\text{model,meta}}$ DNN models as the first-level learner and the meta model as the second-level learner.

Using the training and testing samples, the meta-based ensemble learning architecture is trained to minimize mean squared error. Finally, sigmoid [43] is used as the activation function for the output layer and the Adam optimiser is employed for weight update. The proposed meta model design is described in Table 3.

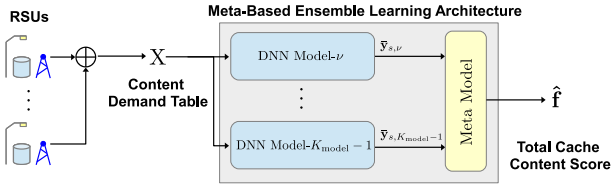

FIGURE 4. An illustration of the proposed MELDEC strategy with the meta-based ensemble learning architecture.

TABLE 3. Meta model design.

Layer	Output Dimensions
Input	$1 \times (K_{\text{model,meta}} \bullet K_{\text{total}})$
Dense + ReLU	32
Dense + ReLU	32
Dense + ReLU	32
Sigmoid	K_{total}

2) OFFLINE TRAINING AND DEPLOYMENT

We adopt similar offline training and deployment steps seen in the ELDEC strategy for the MELDEC strategy. In particular, the $K_{\text{model,meta}}$ DNN models and the meta model in the MELDEC strategy are trained offline with M_{train} samples and validated online with M_{test} samples using the cloud-based deep learning platform. For each of the $K_{\text{model,meta}}$ DNN models, the output and input layers are aggregated and used as the inputs to the meta model and meta-based ensemble learning architecture, respectively. The meta-based ensemble learning architecture is then used for offline training, before $\hat{\mathbf{f}}$ and $\hat{\mathbf{f}}_{\text{cache}}$ are computed with M_{test} samples. The top K_{cache} files with the highest cache content scores in $\hat{\mathbf{f}}$ are then selected to be cached at RSUs, with the corresponding file index populated in $\hat{\mathbf{f}}_{\text{cache}}$. It is worth noting that the estimated cache hit ($P_{\text{hit,MEL}}$) for the MELDEC strategy is obtained using (4). A summary of the offline training and deployment process for the MELDEC strategy is presented in Algorithm 2 and illustrated in Fig. 4.

C. BENCHMARK AND OPTIMAL SCHEMES

We employ the deep learning edge caching (DLEC) strategy in [28] and non learning-based Least Frequently Used

6. The time taken to collect M_{dataset} samples depends on the number of RSUs and CVs in the IoV network due to the frequency of file requests. Thus, popular content prediction and distribution can be conducted more frequently in a larger IoV network compared to a smaller IoV network.

7. It is worth noting that $P_{\text{hit,EL}}$ can be further improved by caching a mix of contents that are popular or have large content diversity in the ELDEC strategy, as was done in [13], which will investigated in future extensions of this paper.

Algorithm 2 MELDEC Offline Training and Deployment

Input: $\mathbf{X}$, $K_{\text{model,meta}}$, M_{test}, M_{train}, K_{total}
Output: $\hat{\mathbf{f}}_{\text{cache}}$

1: Randomly select M_{train} samples from $\mathbf{X}$ for training.
2: Allocate remaining M_{test} samples from $\mathbf{X}$ for validation.
3: **for** $\nu = 0, 1, \ldots, K_{\text{model,meta}} - 1$ **do**
4: Build DNN model-ν using Table 2.
5: **end for**
6: Build meta model using Table 3.
7: Aggregate output layers of all $K_{\text{model,meta}}$ DNN models as the input to the meta model.
8: Aggregate input layers of all $K_{\text{model,meta}}$ DNN models as the input to the meta-based ensemble learning architecture.
9: Train meta-based ensemble learning architecture with M_{train} samples.
10: Compute $\hat{\mathbf{f}}$ and $\hat{\mathbf{f}}_{\text{cache}}$ with the meta-based ensemble learning architecture with M_{test} samples.
11: Populate all RSUs with files indicated in $\hat{\mathbf{f}}_{\text{cache}}$.

(LFU), Least Recently Used (LRU) as the benchmark schemes [44], [45] to benchmark the performance of the proposed MELDEC and ELDEC strategies in the IoV network. We also employ the oracle algorithm as the optimal scheme in this work [44], [45][8,9] In particular, the LFU and LRU schemes respectively removes the least frequently used and least recently used file from the RSUs when the MEC server cache is full. For the oracle algorithm, the popularity of all K_{total} files is assumed to be known a priori [45], i.e., the oracle algorithm is the optimal scheme to determine file popularity. Using (4), we obtain $P_{\text{hit,DL}}$, $P_{\text{hit,LFU}}$, $P_{\text{hit,LRU}}$, and $P_{\text{hit,Oracle}}$ as the estimated cache hit rate for DLEC in [28], LFU, LRU, and the oracle schemes, respectively. The estimated cache hit rate $P_{\text{hit},u}, u \in \{\text{EL, MEL, DL, LFU, LRU, Oracle}\}$ enables closed-form outage probability and finite SNR diversity gain expressions to be derived for the proposed MELDEC strategy, ELDEC strategy, and benchmark schemes, which will be further discussed in subsequent sections.

IV. PERFORMANCE ANALYSIS OF THE IOV NETWORK

In this section, we derive the closed-form outage probability and finite signal-to-noise ratio (SNR) diversity gain expressions in the IoV network.

A. OUTAGE PROBABILITY ANALYSIS

Let τ be the latency to download the requested file from RSUs or cellular BSs to the CV, and $\gamma_{\text{th}} = 2^{\frac{K_{\text{size}}}{\tau B_{\text{w}}}} - 1$ be the threshold [13, eq. (7)]. Then, the outage probability (P_{out}) of the IoV network is given in the following theorem.

Theorem 1: The outage probability of the CV in the IoV network is:

$$P^{u}_{\text{out}} = P_{\text{hit},u}\Bigg[\sum_{p=0}^{\infty}\sum_{q=0}^{m_j+p}\alpha_j(p)\binom{m_j+p}{q}\mathbb{E}\{Z_j^q\} \times \Delta_j(p,q)\Theta_j(p,q)\bar{P}_t^{\,q-(m_j+p)}\Bigg]^{M_{\text{RSU}}} + \left(1-P_{\text{hit},u}\right)\Bigg[\sum_{p=0}^{\infty}\sum_{q=0}^{m_i+p}\alpha_i(p)\binom{m_i+p}{q}\mathbb{E}\{Z_i^q\} \times \Delta_i(p,q)\Theta_i(p,q)\bar{P}_t^{\,q-(m_i+p)}\Bigg]^{M_{\text{BS}}}, \tag{5}$$

where $u \in \{\text{EL, MEL, DL, LFU, LRU, Oracle}\}$, $\alpha_x(p) = \frac{(-1)^p(m_x\gamma_{\text{th}})^{m_x+p}}{\Gamma(m_x)p!(m_x+p)}$, $\mathbb{E}\{Z_x^q\} = \frac{\Gamma(\mu_x+q)}{\Gamma(\mu_x)(\mu_x)^q}$, $\Theta_x(p,q) = \frac{(1-\epsilon^2)^q}{(\epsilon^2)^{m_x+p}}$, and $\Delta_x(p,q) = \frac{2r_a^{l(m_x+p-q)}}{l(m_x+p-q)+2}$.

Proof: The proof is given in Appendix A. ∎

The function $\alpha_x(p)$ represents the power series expansion of the cumulative distribution function (CDF) for the random variable (RV) $|\hat{h}_x|^2, x \in \{i, j\}$, while $\mathbb{E}\{Z_x^q\}$ is the q-th moment of the RV Z [46, Table II]. Also, the function $\Delta_x(p,q)$ accounts for the impact of stochastic geometry on outage probability in the IoV network and $\Theta_x(p,q)$ accounts for the impact of CSI estimation errors on outage probability due to the speed of the CV v and feedback period T. In the next corollary, we show that the closed-form outage probability expression in (5) is convergent.

Corollary 1: The closed-form outage probability expression in (5) has a convergence radius of ∞.

Proof: The proof is given in Appendix B. ∎

At high $\bar{P}_t$ regimes, the asymptotic outage probability ($P_{\text{out},\infty}$) when BS-i and RSU-j of the CV is given in the following corollary.

Corollary 2: The asymptotic outage probability of the CV in the IoV network is:

$$P^{u}_{\text{out},\infty} = P_{\text{hit},u}\Bigg[\sum_{p=0}^{\infty}\alpha_j(p)\mathbb{E}\left\{Z_j^{m_j+p}\right\}\left(\frac{1-\epsilon^2}{\epsilon^2}\right)^{m_j+p}\Bigg]^{M_{\text{RSU}}} + \left(1-P_{\text{hit},u}\right)\Bigg[\sum_{p=0}^{\infty}\alpha_i(p)\mathbb{E}\left\{Z_i^{m_i+p}\right\}\left(\frac{1-\epsilon^2}{\epsilon^2}\right)^{m_i+p}\Bigg]^{M_{\text{BS}}}. \tag{6}$$

Proof: From (5), $\lim_{\bar{P}_t\to\infty}(\bar{P}_t)^{q-m_x-p} = 0$ when $q < m_x + p$ for $x \in \{i, j\}$. For $q = m_x + p$, $\lim_{\bar{P}_t\to\infty}(\bar{P}_t)^{q-m_x-p} = 1$. Therefore, evaluating (5) with $q = m_x+p$ leads to the final expression in (6). This completes the proof. ∎

Remark 1: It is observed through (6) that the random location of the typical CV, i.e., stochastic geometry, in the IoV

8. We choose the work in [28] as one of the benchmark schemes due to the relatively low computational complexity, which makes it suitable for deployment in a practical IoV network.

9. The approaches in [9], [10], [11], [12] may be computationally complex to implement in practice. However, future works will investigate these techniques for benchmarking.

network does not affect $P^u_{\text{out},\infty}$. Instead, the estimated cache hit rate, small-scale fading in the IoV network, and CSI estimation errors due to mobility play a larger role in determining $P^u_{\text{out},\infty}$ regardless of the underlying edge caching strategies employed.

When the feedback period (T) is sufficiently long or when the vehicle speed (v) is adequately low, then one may obtain the ideal CSI estimation, i.e., $\epsilon \approx 1$. In such cases, the outage probability $P^u_{\text{out,Ideal CSI}}$ of the CV can be approximated from (5) as shown in the following corollary.

Corollary 3: The outage probability of the CV when ideal CSI estimation is obtained in the IoV network is:

$$P^u_{\text{out,Ideal CSI}} = P_{\text{hit},u}\left[\sum_{p=0}^{\infty}\alpha_j(p)\Delta_j(p,0)\bar{P}_t^{-(m_j+p)}\right]^{M_{\text{RSU}}} + \left(1-P_{\text{hit},u}\right)\left[\sum_{p=0}^{\infty}\alpha_i(p)\Delta_i(p,0)\bar{P}_t^{-(m_i+p)}\right]^{M_{\text{BS}}}. \tag{7}$$

Proof: We begin by noting that $\Theta_x(p,q) \approx 1$ when $q = 0$, while $\Theta_x(p,q) \approx 0$ when $q > 0$. Therefore, $P^u_{\text{out,Ideal CSI}}$ can be approximated from (5) with $q = 0$ when $\epsilon \approx 1$. Finally, the final expression in (7) is obtained after some algebraic simplifications. This completes the proof. ■

Using (5), (6), and (7), one can evaluate P^u_{out}, $P^u_{\text{out},\infty}$, and $P^u_{\text{out,Ideal CSI}}$, in closed-form, respectively, after obtaining the estimated cache hit rate of the proposed MELDEC strategy, ELDEC strategy, or any of the benchmark schemes, i.e., $P_{\text{hit},u}$ where $u \in \{\text{EL, MEL, DL, LFU, LRU, Oracle}\}$. Additionally, one will be able to evaluate any edge caching strategy with the closed-form expressions in (5), (6), and (7), as long as the estimated cache hit rate is obtainable.

B. FINITE SNR DIVERSITY GAIN ANALYSIS

In wireless networks operating at low to moderate SNR regimes, the outage probability decay is quantified through the finite SNR diversity gain d_f [22], [23]. Specifically, finite SNR diversity gain is defined as [22, eq. (5)]:

$$d_f = \frac{-P_r}{Pr(\mathcal{O})}\frac{\partial}{\partial P_r}Pr(\mathcal{O}), \tag{8}$$

where $\mathcal{O}$, $Pr(\mathcal{O})$, and P_r are the outage event, outage probability, and average received power in the considered wireless network, respectively. Using d_f, one also obtains the diversity gain at asymptotic SNRs by evaluating (8) at high SNR regimes [23], [47], [48]. To this end, we employ finite SNR analysis to investigate the outage probability decay in the IoV network.

Let the finite SNR diversity gain of the CV in the IoV network be d^u_f, where $u \in \{\text{EL, MEL, DL, LFU, LRU, Oracle}\}$. Then, d^u_f is given in the following proposition.

Proposition 1: The finite SNR diversity gain of the CV in the IoV network is:

$$\begin{aligned} d^u_f = \frac{-\bar{P}_t}{P^u_{\text{out}}}\Bigg(& P_{\text{hit},u}M_{\text{RSU}}\Bigg[\sum_{p=0}^{\infty}\sum_{q=0}^{m_j+p}\alpha_j(p)\binom{m_j+p}{q}\mathbb{E}\{Z_j^q\} \\ &\times \Delta_j(p,q)\Theta_j(p,q)\bar{P}_t^{\,q-(m_j+p)}\Bigg]^{M_{\text{RSU}}-1} \\ &\times\Bigg[\sum_{p=0}^{\infty}\sum_{q=0}^{m_j+p}\alpha_j(p)\binom{m_j+p}{q}\mathbb{E}\{Z_j^q\}\Delta_j(p,q) \\ &\times\Theta_j(p,q)\big(q-(m_j+p)\big)\bar{P}_t^{\,q-(m_j+p)-1}\Bigg] \\ &+\left(1-P_{\text{hit},u}\right)M_{\text{BS}}\Bigg[\sum_{p=0}^{\infty}\sum_{q=0}^{m_i+p}\alpha_i(p)\binom{m_i+p}{q}\mathbb{E}\{Z_i^q\} \\ &\times\Delta_i(p,q)\Theta_i(p,q)\bar{P}_t^{\,q-(m_i+p)}\Bigg]^{M_{\text{BS}}-1} \\ &\times\Bigg[\sum_{p=0}^{\infty}\sum_{q=0}^{m_i+p}\alpha_i(p)\binom{m_i+p}{q}\mathbb{E}\{Z_i^q\}\Delta_i(p,q) \\ &\times\Theta_i(p,q)(q-(m_i+p))\bar{P}_t^{\,q-(m_i+p)-1}\Bigg]\Bigg). \end{aligned} \tag{9}$$

Proof: The finite SNR diversity gain of the CV is obtained by substituting (5) into (8). ■

Using (9), the diversity gain of the CV, i.e., decay of P^u_{out}, can be analzyed at low-to-medium SNR regimes. Specifically, the impact of the estimated cache hit rate ($P_{\text{hit},u}$), small-scale fading, and CSI estimation error on outage behavior in the IoV network can be observed using (9), which would otherwise not be present at high SNR regimes. To see this, the asymptotic diversity gain of the CV in the IoV network is presented in the next corollary.

Corollary 4: The asymptotic diversity gain of the CV in the IoV network is:

$$\lim_{\bar{P}_t\to\infty} d^u_f = 0. \tag{10}$$

Proof: We begin by noting that $\lim_{\bar{P}_t\to\infty} d^u_f$ can be expressed as:

$$\lim_{\bar{P}_t\to\infty} d^u_f = \frac{-\bar{P}_t}{P^u_{\text{out},\infty}}\frac{\partial}{\partial\bar{P}_t}P^u_{\text{out},\infty}. \tag{11}$$

From (6), it is seen that $P^u_{\text{out},\infty}$ is independent of $\bar{P}_t$. Therefore, $\frac{-\bar{P}_t}{P^u_{\text{out},\infty}}\frac{\partial}{\partial\bar{P}_t}P^u_{\text{out},\infty}$ evaluates to zero, which completes the proof. ■

The result in Corollary 4 is due to the fact that at high SNR regimes, the instantaneous SINR $\gamma_x, x \in \{i,j\}$ becomes limited by interference due to CSI estimation errors as a result of mobility. Thus, increasing $\bar{P}_t$ corresponds to negligible decrease in outage probability at the CV.

For scenarios where ideal CSI estimation is obtained, the closed-form finite SNR diversity gain $d^u_{f,\text{Ideal CSI}}$ expression is presented in the following proposition.

Proposition 2: When ideal CSI estimation is attained, the finite SNR diversity gain of the CV in the IoV network is:

$$d^{u}_{f,\text{Ideal CSI}} = \frac{-\bar{P}_t}{P^{u}_{\text{out,Ideal CSI}}} \times \Bigg(P_{\text{hit},u} M_{\text{RSU}} \Bigg[\sum_{p=0}^{\infty} \alpha_j(p) \Delta_j(p,0) \bar{P}_t^{-(m_j+p)} \Bigg]^{M_{\text{RSU}}-1} \times \Bigg[\sum_{p=0}^{\infty} \alpha_j(p) \Delta_j(p,0) (-m_j - p) \bar{P}_t^{-(m_j+p+1)} \Bigg] + (1 - P_{\text{hit},u}) M_{\text{BS}} \Bigg[\sum_{p=0}^{\infty} \alpha_i(p) \Delta_i(p,0) \bar{P}_t^{-(m_i+p)} \Bigg]^{M_{\text{BS}}-1} \times \Bigg[\sum_{p=0}^{\infty} \alpha_i(p) \Delta_i(p,0) (-m_i - p) \bar{P}_t^{-(m_i+p+1)} \Bigg] \Bigg). \tag{12}$$

Proof: The finite SNR diversity gain in (12) is obtained by substituting (7) into (8). ■

At high SNR regimes, the asymptotic behavior of $d^{u}_{f,\text{Ideal CSI}}$ is presented in the following corollary.

Corollary 5: When ideal CSI estimation is attained, the asymptotic diversity gain of the CV in the IoV network is approximated as:

$$\lim_{\bar{P}_t \to \infty} d^{u}_{f,\text{Ideal CSI}} \approx \min \Big(M_{\text{RSU}} m_j, M_{\text{BS}} m_i \Big). \tag{13}$$

Proof: The proof is given in Appendix C. ■

Remark 2: It is worth emphasizing the main reason behind adopting the BPP over the PPP in this paper lies in the fact that the number of RSUs and cellular BSs simulated in PPPs is a random variable. As such, assuming PPPs in the IoV network may not lead to a tractable outage and finite SNR analysis. This is in contrast to the BPP, which allows one to investigate the exact relationship between M_{RSU} and M_{BS}, and its impact on outage probability and diversity gain in the IoV network as shown in (5)-(13). Furthermore, the closed-form expressions and resulting corollaries seen in this section are possible due to the BPP assumption adopted in this paper. This is in contrast to the PPP assumption, which has been widely adopted to model the random spatial locations of traffic infrastructure in vehicular networks, e.g., [5].

Corollary 5 shows that under high SNR regimes and ideal CSI estimation, the estimated cache hit rate of the proposed MELDEC strategy, ELDEC strategy, and the benchmark schemes do not influence the diversity gain of the CV. Instead, the diversity gain is determined based on the number of cellular BSs (M_{BS}) and RSUs (M_{RSU}), and the severity of Nakagami-m fading ($m_x, x \in \{i, j\}$) experienced in the IoV network. Using (12), (13) describes the relationship between M_{BS}, M_{RSU}, $m_x, x \in \{i, j\}$, and the diversity gain under high SNR regimes and ideal CSI estimation in closed-form.

V. NUMERICAL AND SIMULATION RESULTS

In this section, numerical results pertaining to the performance of the MELDEC and ELDEC strategies in the IoV network are presented, with Monte Carlo simulations conducted with 10^5 samples. We also provide the default simulation parameters in Table 4.

TABLE 4. Default simulation parameters.

Parameter(s)	Value(s)
File Popularity Factor	$z = 1.01$
Total Files	$K_{\text{total}} = 5000$
File Size	$K_{\text{size}} = 30$ MB [49]
RSU Cache Size	$K_{\text{cache}} = 600$
Number of DNN Models	$K_{\text{model}} = 5$, $K_{\text{model,meta}} = 5$
Carrier Frequency	$f_c = 5.9$ GHz [39]
Bandwidth	$B_{\text{w}} = 10$ MHz [39]
Number of RSUs and BSs	$M_{\text{RSU}} = 20$, $M_{\text{BS}} = 3$
Transmit Power	$P_t = 20$ dBm [31]
Path Loss, Path Loss Exponent	$L_0 = 47.86$ dB [39], $l = 2$ [31]
Feedback Period, Vehicle Speed	$T = 0.5$ ms [30], $v = 40$ km/h
Transmission rate, Latency	$R = 3.1$ b/s/Hz, $\tau = 7.74$s
Radius	$r_a = 500$m
Nakagami-m fading parameters	$m_x = \mu_x = 2, x \in \{i, j\}$

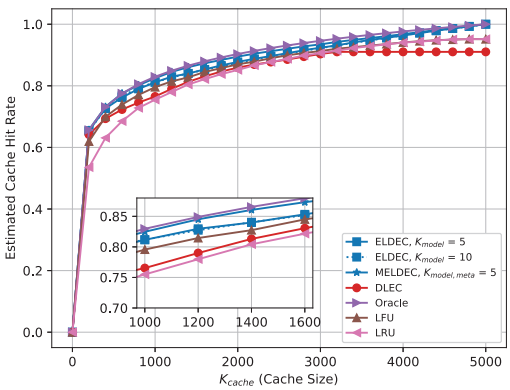

FIGURE 5. A comparison of the estimated cache hit rates for the proposed MELDEC strategy, ELDEC strategy, and benchmark schemes.

A. ESTIMATED CACHE HIT RATE AND RUN TIME ANALYSIS

We train the MELDEC strategy, ELDEC strategy, and benchmark schemes with the content demand table $\mathbf{X}$ using $M_{\text{dataset}} = 10^5$ rows, and generate a new content demand table $\mathbf{X}_{\text{eval}}$ with 10^5 rows which are populated independently from $\mathbf{X}$. The evaluation of the estimated cache hit rate ($P_{\text{hit,u}}$), $u \in \{\text{EL, MEL, DL, LFU, LRU, Oracle}\}$ for the MELDEC strategy, ELDEC strategy, and benchmark schemes is then conducted using $\mathbf{X}_{\text{eval}}$, where $P_{\text{hit,u}}$ is obtained with $\mathbf{X}$ and validated using $\mathbf{X}_{\text{eval}}$.

Fig. 5 shows the comparison of $P_{\text{hit,u}}, u \in \{\text{EL, MEL, DL, LFU, LRU, Oracle}\}$ as cache size (K_{cache}) increases. It is seen that the proposed MELDEC strategy outperforms the ELDEC strategy and the benchmark schemes, and that similar $P_{\text{hit,EL}}$ is obtained when $K_{\text{model}} \in \{5, 10\}$. It is also observed that the proposed MELDEC strategy achieves near-optimal cache hit rates, i.e., $P_{\text{hit,MEL}}$ is close to $P_{\text{hit,Oracle}}$. Similar to the optimal oracle algorithm, the proposed MELDEC and ELDEC strategies are also able to achieve 100% $P_{\text{hit,EL}}$ and 100% $P_{\text{hit,MEL}}$ when $K_{\text{cache}} = 5000$, i.e., when RSUs cache all K_{total} files. In

TABLE 5. Run time comparison.

Method	Comments	Run Time (s)
ELDEC	$K_{\text{model}} = 5$.	1.4s
ELDEC	$K_{\text{model}} = 10$.	2.8s
MELDEC	$K_{\text{model,meta}} = 5$.	0.7s
DLEC	As described in [28].	0.3s
LFU	As described in [44], [45].	112s
LRU	As described in [44], [45].	95.2s

contrast, it is seen that the DLEC strategy achieves $P_{\text{hit,DL}}$ that is less than the LFU scheme but higher than the LRU scheme at low K_{cache}, i.e., $K_{\text{cache}} < 1400$. Furthermore, it is noted that the benchmark schemes exhibit a plateauing cache hit rate at high K_{cache}, e.g., $K_{\text{cache}} > 4200$ for the LFU and LRU schemes and $K_{\text{cache}} > 3200$ for the DLEC strategy. Similar trends have also been observed in [44, Fig. 3] and [26, Fig. 12], and this is due to the fact that the benchmark schemes are limited by the distribution of the underlying file popularity [44]. Specifically, the LFU and LRU schemes cache contents by reacting to file requests from CVs in the IoV network. For files which are requested for the first time, a cache miss is still recorded despite $K_{\text{cache}} = K_{\text{total}} = 5000$ since the requested file has not been cached at the start. For the DLEC strategy, contents are cached based on predicted content popularity. As a result, the DLEC strategy may not cache files which were not requested during dataset collection despite $K_{\text{cache}} = K_{\text{total}} = 5000$.

A comparison of the run time for the MELDEC strategy, ELDEC strategy, and benchmark schemes is provided in Table 5.[10] We define the run time as the total time taken to run the ELDEC strategy and the benchmark schemes for content popularity prediction over M_{test} test samples. The run times of the MELDEC strategy, ELDEC strategy, and benchmark schemes are obtained using the same Intel Core i7-1165G7 processor with multi-core processing disabled to ensure that a single core is used during simulations.[11] As with [25], [50], the MELDEC, ELDEC, and DLEC run times do not account for the training time as the training for both strategies in this paper are conducted offline. From Table 5, it is seen that the DLEC strategy exhibits a shorter run time than the MELDEC, ELDEC, LFU, and LRU schemes. The MELDEC strategy is also noted to have 50% shorter run time than the ELDEC strategy. Furthermore, we observed that the MELDEC and ELDEC strategies achieve a shorter run time as the LFU and LRU schemes. Although MELDEC and ELDEC have longer run times than DLEC, $P_{\text{hit,EL}}$ and $P_{\text{hit,MEL}}$ are considerably higher than the benchmark schemes and is near-optimal when compared to the oracle algorithm. In practice, the run time of the MELDEC and ELDEC strategies can be reduced by utilizing parallel computing platforms such as graphic processing units (GPUs) in IoV networks.[12]

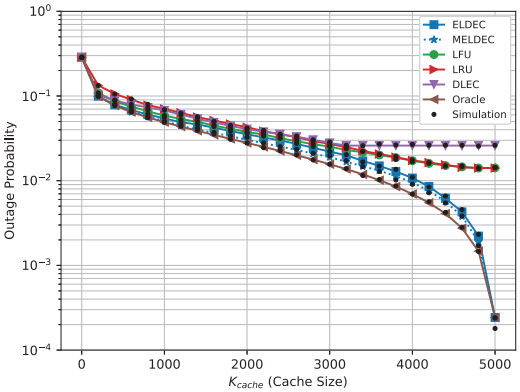

FIGURE 6. The impact of K_{cache} on the outage probability of the proposed MELDEC strategy, ELDEC strategy, and benchmark schemes.

B. OUTAGE PROBABILITY AND FINITE SNR ANALYSIS

The impact of K_{cache} on outage probability is shown in Fig. 6 for the proposed MELDEC strategy, ELDEC strategy, and benchmark schemes. When K_{cache} is small, e.g., $K_{\text{cache}} < 200$, the estimated cache hit rate $P_{\text{hit,u}}, u \in \{\text{EL, MEL, DL, LFU, LRU, Oracle}\}$ for the MELDEC strategy, ELDEC strategy, and benchmark schemes is low due to the limited availability of cache storage at RSUs. In turn, the outage probability P_{out}^{u} becomes limited by the associated cellular BS link of the CV. As K_{cache} increases, a higher $P_{\text{hit,u}}$ ensues due to a greater availability of cache storage at the RSUs. As a result, the outage probability P_{out}^{u} improves and becomes increasingly influenced by the respective estimated cache hit rate $P_{\text{hit,u}}$ for the MELDEC strategy, ELDEC strategy, and benchmark schemes. Specifically, this can be observed at high K_{cache} where the outage probability of the benchmark schemes plateaus, e.g., $K_{\text{cache}} > 3000$. Such an observation is due to the fact that $P_{\text{hit,DL}}$, $P_{\text{hit,LFU}}$, and $P_{\text{hit,LFU}}$ also begins to plateau when $K_{\text{cache}} > 3000$, which can also be seen in Fig. 5. Likewise, a lower outage probability is attained when employing the proposed MELDEC and ELDEC strategies due to higher $P_{\text{hit,EL}}$ and $P_{\text{hit,MEL}}$ (as seen in Fig. 5). As such, Fig. 6 shows that the choice of K_{cache} greatly influences P_{out}^{u} in the IoV network.

In Fig. 7, the impact of transmit power (P_t) on outage probability and diversity gain is seen for low-to-high SNR regimes. It is seen in Fig. 7(a) that $P_{\text{out}}^{\text{LFU}} < P_{\text{out}}^{\text{DL}} < P_{\text{out}}^{\text{LRU}}$, as $P_{\text{hit,LFU}} > P_{\text{hit,DL}} > P_{\text{hit,LRU}}$ for $K_{\text{cache}} = 600$ (Fig. 5).

10. We omit the run time attained by the oracle algorithm, as it is unrealisable in practice due to the assumption that content popularity is known a priori.

11. Similar to [25], [50], the run time across the MELDEC strategy, ELDEC strategy, and benchmark schemes is chosen as the main metric for complexity analysis in this work. This is because evaluating the number of floating point operations across all schemes may not lead to a fair comparison, since both the LFU and LRU schemes are iterative in nature when compared to the ELDEC and DLEC strategies. Furthermore, popular deep learning libraries, e.g., TensorFlow, have also been optimized for deep learning implementation [25].

12. It is worth noting that the authors in [25] have similarly proposed using GPUs to reduce the run time of deep learning-based power control in wireless networks.

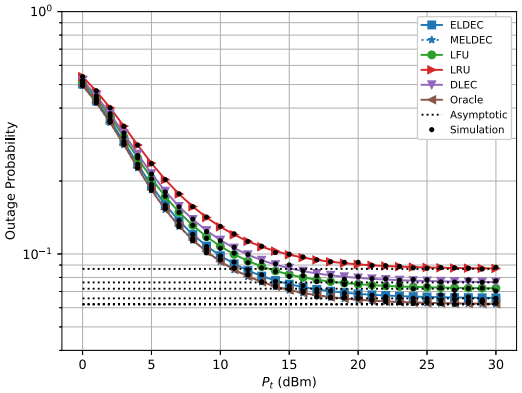

(a) Outage Probability.

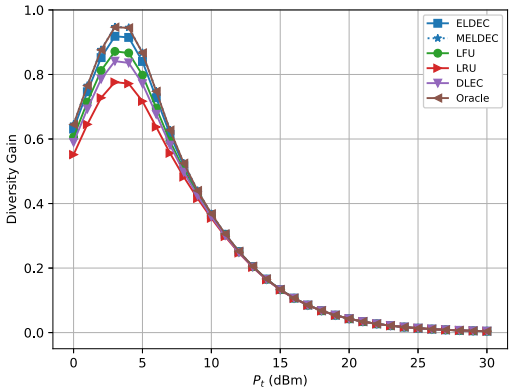

(b) Finite SNR Diversity Gain.

FIGURE 7. The impact of P_t on the outage probability and finite SNR diversity gain of the proposed MELDEC strategy, ELDEC strategy, and benchmark schemes.

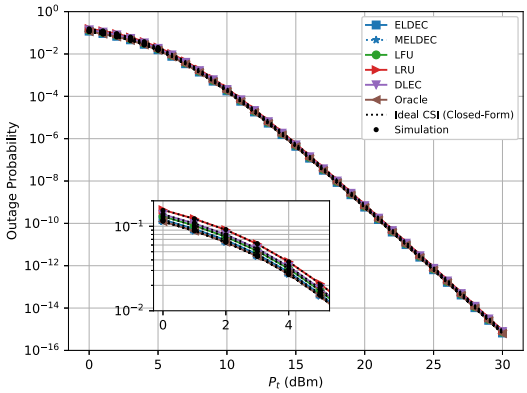

(a) Outage Probability.

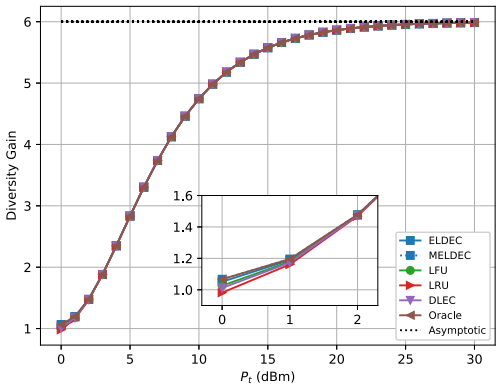

(b) Finite SNR Diversity Gain.

FIGURE 8. The impact of P_t on the outage probability and finite SNR diversity gain of the proposed MELDEC strategy, ELDEC strategy, and benchmark schemes when ideal CSI estimation is attained.

More importantly, it is observed that $P_{\text{out}}^{\text{EL}}$ and $P_{\text{out}}^{\text{MEL}}$ are close to $P_{\text{out}}^{\text{Oracle}}$ for 0 dBm $\leq P_t \leq$ 30 dBm. Corollary 2 is also validated, as it is seen that $P_{\text{out}}^{u} \to P_{\text{out},\infty}^{u}$ when $P_t \to$ 30 dBm. In Fig. 7(b), it is observed that the diversity gains (d_f^u) of the MELDEC strategy, ELDEC strategy, and benchmark schemes peak at $P_t = 3$ dBm before gradually decreasing as P_t increases. This can also be observed in Fig. 7(a), where P_{out}^{u} decays rapidly at low P_t regimes before the decay rate becomes negligible at high P_t regimes. Furthermore, Corollary 4 is validated as it is seen that $d_f^u \to 0$ when $P_t \to$ 30 dBm. Thus, Fig. 7 demonstrates that the proposed MELDEC and ELDEC strategies are capable of achieving near-optimal outage probability and finite SNR diversity gain in the IoV network.

In Fig. 8, the impact of P_t on outage probability and diversity gain under ideal CSI estimation is seen for low-to-high SNR regimes. In particular, it is seen in Fig. 8(a) that the MELDEC strategy, ELDEC strategy, and benchmark schemes achieve similar outage probability $P_{\text{out,Ideal CSI}}^{u}$ when 0 dBm $\leq P_t \leq$ 30 dBm, with $P_{\text{out,Ideal CSI}}^{\text{LFU}} < P_{\text{out,Ideal CSI}}^{\text{DL}} < P_{\text{out,Ideal CSI}}^{\text{LRU}}$. Furthermore, it is noted that $P_{\text{out,Ideal CSI}}^{\text{EL}}$ and $P_{\text{out,Ideal CSI}}^{\text{MEL}}$ are close to $P_{\text{out,Ideal CSI}}^{\text{Oracle}}$. In Fig. 8(b), it is seen that the MELDEC strategy, ELDEC strategy, and the benchmark schemes attain similar $d_{f,\text{Ideal CSI}}^{u}$ when 0 dBm $\leq P_t \leq$ 30 dBm. Such a trend is also noted in Fig. 8(a) where the respective decay rate of $P_{\text{out,Ideal CSI}}^{u}$ for the MELDEC strategy, ELDEC strategy, and benchmark schemes remain largely similar for 0 dBm $\leq P_t \leq$ 30 dBm. As $P_t \to$ 30 dBm, Corollary 5 is validated since it is observed that $d_{f,\text{Ideal CSI}}^{u} \approx \min(M_{\text{RSU}} m_j, M_{\text{BS}} m_i)$. Evidently, Fig. 8 shows that the impact of the estimated cache hit rate $P_{\text{hit,u}}$ on outage probability and diversity gain is greatly diminished when ideal CSI estimation is attained.[13] Instead, we demonstrate through Corollary 5 that the number of cellular BSs and RSUs, along with the severity of Nakagami-m fading in the IoV network, largely determine the outage probability and diversity gain at the CV under ideal CSI estimation.

VI. CONCLUSION AND FUTURE RESEARCH DIRECTIONS

An ELDEC strategy that incorporates ensemble learning and an MELDEC strategy which combines meta and ensemble learning is proposed in this paper for content popularity prediction and cache content placement in IoV networks. Specifically, closed-form outage probability and finite SNR diversity gain expressions are derived for the performance

13. Such scenarios can occur in practice when CVs in an IoV network are stationary at traffic junctions.

characterization of the MELDEC strategy, ELDEC strategy, and benchmark schemes. Through a comprehensive analysis, we show that the proposed MELDEC strategy and ELDEC strategy achieve near-optimal cache hit rates, outage probability, and finite SNR diversity gain when compared to the benchmark schemes under imperfect CSI estimation scenarios. It is also demonstrated that the finite SNR diversity gain under ideal CSI estimation is independent of the estimated cache hit rates of the MELDEC strategy, ELDEC strategy, and benchmark schemes. Instead, we reveal through finite SNR analysis that the finite SNR diversity gain under ideal CSI estimation is dependent on the number of cellular BSs and RSUs, and the severity of Nakagami-m fading in the IoV network. The near-optimal performance of the MELDEC and ELDEC strategies demonstrate both as viable solutions for deep learning-based edge caching in IoV networks.

Nevertheless, enhancing the content popularity prediction accuracy, i.e., cache hit rate, of both MELDEC and ELDEC strategies remains an open challenge. Specifically, the cache hit rates of both the MELDEC and ELDEC strategies can be potentially improved by considering other temporal factors, e.g., CV mobility and content lifespan. Thus, a redesign of the content demand table to properly consider temporal factors together with content access rates is proposed as part of future directions of this study. Additionally, the performance of content popularity prediction for both MELDEC and ELDEC strategies can be improved by incorporating elements of distributed learning and cooperative-based vehicle-to-vehicle communications. Hence, enhancing the MELDEC and ELDEC strategies with distributed learning and cooperative methods while mitigating the associated high overheads and handovers is also proposed as part of future research directions of this study.

APPENDIX A
PROOF OF (5)

We begin by first noting that an outage occurs in the IoV network when the CV is unable to download the requested file from the associated RSU and cellular BS. Hence, the outage probability (P_{out}) is defined as:

$$P^{u}_{\text{out}} = P_{\text{hit},u}\mathbb{P}\left(\max_{1\le j\le M_{\text{RSU}}}\left(\gamma_j\right) \le \gamma_{\text{th}}\right) + \left(1-P_{\text{hit},u}\right)\mathbb{P}\left(\max_{1\le i\le M_{\text{BS}}}\left(\gamma_i\right) \le \gamma_{\text{th}}\right), \quad (14)$$

where i and j are the indices of the associated cellular BS and RSU, respectively. The first term in (14) occurs if the requested file is available at RSU-j, while the second term in (14) occurs if the file is only available at BS-i.

Since cellular links experience Nakagami-m fading, the outage probability conditioned on d_i and d_j can be written as [27], [46]:

$$P^{u}_{\text{out}|d_i,d_j} = P_{\text{hit},u}\left[\mathbb{E}\left\{F_{|\hat{h}_j|^2}\left(\gamma_{\text{th}}\left[1+|e_j|^2 d_j^{-l}\right]d_j^{l}\right)\middle| d_j\right\}\right]^{M_{\text{RSU}}} + \left(1-P_{\text{hit},u}\right)\left[\mathbb{E}\left\{F_{|\hat{h}_i|^2}\left(\gamma_{\text{th}}\left[1+|e_i|^2 d_i^{-l}\right]d_i^{l}\right)\middle| d_i\right\}\right]^{M_{\text{BS}}}, \quad (15)$$

where $F_{|\hat{h}_x|^2}(\cdot), x\in\{i,j\}$ is the CDF of $|\hat{h}_x|^2$.

Thereafter, we apply the techniques in [27, Lemma 1] and [46, Th. 1] to express (15) as:

$$P^{u}_{\text{out}|d_i,d_j} = P_{\text{hit},u}\left[\sum_{p=0}^{\infty}\sum_{q=0}^{m_j+p}\alpha_j(p)\binom{m_j+p}{q}\frac{\mathbb{E}\{Z_j^q\}\Theta_j(p,q)}{\left(\bar{P}_t d_j^{-l}\right)^{(m_j+p-q)}}\right]^{M_{\text{RSU}}} + \left(1-P_{\text{hit},u}\right)\left[\sum_{p=0}^{\infty}\sum_{q=0}^{m_i+p}\alpha_i(p)\binom{m_i+p}{q}\frac{\mathbb{E}\{Z_i^q\}\Theta_i(p,q)}{\left(\bar{P}_t d_i^{-l}\right)^{(m_i+p-q)}}\right]^{M_{\text{BS}}}. \quad (16)$$

Finally, averaging P_{out} over the PDFs of d_i and d_j yields (5). This completes the proof.

APPENDIX B
PROOF OF CONVERGENCE FOR (5)

We begin the proof by letting $y_x(p,q) = \alpha_x(p)\binom{m_x+p}{q}\mathbb{E}\{Z_x^q\}\Delta_x(p,q)\Theta_x(p,q)\bar{P}_t^{\,q-(m_x+p)}$, where $x\in\{i,j\}$. Then, (5) can be rewritten as:

$$P^{u}_{\text{out}} = P_{\text{hit},u}\left[\sum_{p=0}^{\infty}\sum_{q=0}^{m_j+p} y_j(p,q)\right]^{M_{\text{RSU}}} + \left(1-P_{\text{hit},u}\right)\left[\sum_{p=0}^{\infty}\sum_{q=0}^{m_i+p} y_i(p,q)\right]^{M_{\text{BS}}}, \quad (17)$$

To prove the convergence of (5), we need to show that the power series expressions in (17) are convergent. Invoking the D'Alembert test, $\lim_{p\to\infty}\frac{|y_x(p+1,q)|}{|y_x(p,q)|}$ is evaluated as:

$$\begin{aligned}
&\lim_{p\to\infty}\frac{|y_x(p+1,q)|}{|y_x(p,q)|}\\
&= \lim_{p\to\infty}\frac{\binom{m_x+p+1}{q}p!(m_x+p)m_x\gamma_{\text{th}}}{\binom{m_x+p}{q}(p+1)!(m_x+p+1)\epsilon^2\bar{P}_t}\\
&\quad\times\frac{(l(m_x+p-q)+2)r_a^l}{l(m_x+p+1-q)+2}\\
&\overset{(a)}{=}\lim_{p\to\infty}\frac{m_x\gamma_{\text{th}}r_a^l\left[l(m_x+p-q)+2\right](m_x+p)}{\epsilon^2\bar{P}_t\left[l(m_x+p+1-q)+2\right](m_x+p+1)p}\\
&= \lim_{p\to\infty}\frac{m_x\gamma_{\text{th}}r_a^l}{\epsilon^2\bar{P}_t}\left[1-\frac{1}{m_x+p-q+\frac{2}{l}+1}\right]\\
&\quad\times\left[1-\frac{1}{m_x+p+1}\right]\left(\frac{1}{p}\right)\\
&= 0,
\end{aligned} \quad (18)$$

where (a) is obtained using [38, eq. (6.1.15)] and the asymptotic identity $\Gamma[m+n]\approx m^n\Gamma[m]$ in [46, eq. (25)].

Thus, using (18), (5) has a convergence radius of ∞. Therefore, (5) is shown to be convergent. This completes the proof.

APPENDIX C
PROOF OF (5)

We begin by noting that when evaluating $\lim_{\bar{P}_t\to\infty} d^u_{f,\text{Ideal CSI}}$, only $p = 0$ needs to be considered since $\lim_{\bar{P}_t\to\infty} \bar{P}_t^{-(m_x+p+n)} = 0$ when $x \in \{i, j\}$ and $n \geq 0$. Therefore, $\lim_{\bar{P}_t\to\infty} d^u_{f,\text{Ideal CSI}}$ can be approximated as:

$$\begin{aligned}
&\lim_{\bar{P}_t\to\infty} d^u_{f,\text{Ideal CSI}} \\
&\approx \lim_{\bar{P}_t\to\infty} \Bigg(P_{\text{hit},u} M_{\text{RSU}} m_j \left[\alpha_j(0)\Delta_j(0,0)\bar{P}_t^{-m_j}\right]^{M_{\text{RSU}}} \\
&\quad + \left(1 - P_{\text{hit},u}\right) M_{\text{BS}} m_i \left[\alpha_i(0)\Delta_i(0,0)\bar{P}_t^{-m_i}\right]^{M_{\text{BS}}} \Bigg) \\
&\Big/ \Bigg(P_{\text{hit},u} \left[\alpha_j(0)\Delta_j(0,0)\bar{P}_t^{-m_j}\right]^{M_{\text{RSU}}} \\
&\quad + \left(1 - P_{\text{hit},u}\right) \left[\alpha_i(0)\Delta_i(0,0)\bar{P}_t^{-m_i}\right]^{M_{\text{BS}}} \Bigg) \\
&= \frac{M_{\text{RSU}} m_j}{1 + \frac{\left(1-P_{\text{hit},u}\right)\left[\alpha_i(0)\Delta_i(0,0)\right]^{M_{\text{BS}}}}{P_{\text{hit},u}\left[\alpha_j(0)\Delta_j(0,0)\right]^{M_{\text{RSU}}}} \lim_{\bar{P}_t\to\infty} \bar{P}_t^{M_{\text{RSU}}m_j - M_{\text{BS}}m_i}} \\
&\quad + \frac{M_{\text{BS}} m_i}{1 + \frac{P_{\text{hit},u}\left[\alpha_j(0)\Delta_j(0,0)\right]^{M_{\text{RSU}}}}{\left(1-P_{\text{hit},u}\right)\left[\alpha_i(0)\Delta_i(0,0)\right]^{M_{\text{BS}}}} \lim_{\bar{P}_t\to\infty} \bar{P}_t^{M_{\text{BS}}m_i - M_{\text{RSU}}m_j}}
\end{aligned} \tag{19}$$

Thereafter, evaluating the limits in (19) for $M_{\text{RSU}}m_j < M_{\text{BS}}m_i$ and $M_{\text{RSU}}m_j > M_{\text{BS}}m_i$ yields (13). This completes the proof.

REFERENCES

[1] M. Hartwig, "Connected car. Its history, stages and terms," BMW, Munich, Germany, Rep., 2020. [Online]. Available: https://www.bmw.com/en/innovation/ebook-self-driving-cars-opportunities-for-sustainable-mobility.html

[2] H. Zhou, W. Xu, J. Chen, and W. Wang, "Evolutionary V2X technologies toward the Internet of Vehicles: Challenges and opportunities," *Proc. IEEE*, vol. 108, no. 2, pp. 308–323, Feb. 2020.

[3] X. Pei, H. Yu, X. Wang, Y. Chen, M. Wen, and Y.-C. Wu, "NOMA-based pervasive edge computing: Secure power allocation for IoV," *IEEE Trans. Ind. Informat.*, vol. 17, no. 7, pp. 5021–5030, Jul. 2021.

[4] S. Gurugopinath, P. C. Sofotasios, Y. Al-Hammadi, and S. Muhaidat, "Cache-aided non-orthogonal multiple access for 5G-enabled vehicular networks," *IEEE Trans. Veh. Technol.*, vol. 68, no. 9, pp. 8359–8371, Sep. 2019.

[5] S. Fatahi-Bafqi, Z. Zeinalpour-Yazdi, and A. Asadi, "Analytical framework for mmWave-enabled V2X caching," *IEEE Trans. Veh. Technol.*, vol. 70, no. 1, pp. 585–599, Jan. 2021.

[6] A. Liu and V. K. N. Lau, "Exploiting base station caching in MIMO cellular networks: Opportunistic cooperation for video streaming," *IEEE Trans. Signal Process.*, vol. 63, no. 1, pp. 57–69, Jan. 2015.

[7] S. Chai and V. K. N. Lau, "Online trajectory and radio resource optimization of cache-enabled UAV wireless networks with content and energy recharging," *IEEE Trans. Signal Process.*, vol. 68, pp. 1286–1299, Feb. 2020.

[8] H. T. Nguyen, H. D. Tuan, T. Q. Duong, H. V. Poor, and W.-J. Hwang, "Nonsmooth optimization algorithms for multicast beamforming in content-centric fog radio access networks," *IEEE Trans. Signal Process.*, vol. 68, pp. 1455–1469, Jan. 2020.

[9] Z. Su, Y. Hui, Q. Xu, T. Yang, J. Liu, and Y. Jia, "An edge caching scheme to distribute content in vehicular networks," *IEEE Trans. Veh. Technol.*, vol. 67, no. 6, pp. 5346–5356, Jun. 2018.

[10] L. T. Tan, R. Q. Hu, and L. Hanzo, "Twin-timescale artificial intelligence aided mobility-aware edge caching and computing in vehicular networks," *IEEE Trans. Veh. Technol.*, vol. 68, no. 4, pp. 3086–3099, Apr. 2019.

[11] G. Qiao, S. Leng, S. Maharjan, Y. Zhang, and N. Ansari, "Deep reinforcement learning for cooperative content caching in vehicular edge computing and networks," *IEEE Internet Things J.*, vol. 7, no. 1, pp. 247–257, Jan. 2020.

[12] A. Ndikumana, N. H. Tran, D. H. Kim, K. T. Kim, and C. S. Hong, "Deep learning based caching for self-driving cars in multi-access edge computing," *IEEE Trans. Intell. Transp. Syst.*, vol. 22, no. 5, pp. 2862–2877, May 2021.

[13] Z. Chen, J. Lee, T. Q. S. Quek, and M. Kountouris, "Cooperative caching and transmission design in cluster-centric small cell networks," *IEEE Trans. Wireless Commun.*, vol. 16, no. 5, pp. 3401–3415, May 2017.

[14] S. H. Chae, T. Q. S. Quek, and W. Choi, "Content placement for wireless cooperative caching helpers: A tradeoff between cooperative gain and content diversity gain," *IEEE Trans. Wireless Commun.*, vol. 16, no. 10, pp. 6795–6807, Oct. 2017.

[15] W. Wu, N. Zhang, N. Cheng, Y. Tang, K. Aldubaikhy, and X. Shen, "Beef up mmWave dense cellular networks with D2D-assisted cooperative edge caching," *IEEE Trans. Veh. Technol.*, vol. 68, no. 4, pp. 3890–3904, Apr. 2019.

[16] C. Fan, T. Zhang, Y. Liu, and Z. Zeng, "Cache-enabled HetNets with limited backhaul: A stochastic geometry model," *IEEE Trans. Commun.*, vol. 68, no. 11, pp. 7007–7022, Nov. 2020.

[17] N. Garg, M. Sellathurai, V. Bhatia, and T. Ratnarajah, "Function approximation based reinforcement learning for edge caching in massive MIMO networks," *IEEE Trans. Commun.*, vol. 69, no. 4, pp. 2304–2316, Apr. 2021.

[18] N. Garg, M. Sellathurai, V. Bhatia, B. N. Bharath, and T. Ratnarajah, "Online content popularity prediction and learning in wireless edge caching," *IEEE Trans. Commun.*, vol. 68, no. 2, pp. 1087–1100, Feb. 2020.

[19] Z. Liu, H. Song, and D. Pan, "Distributed video content caching policy with deep learning approaches for D2D communication," *IEEE Trans. Veh. Technol.*, vol. 69, no. 12, pp. 15644–15655, Dec. 2020.

[20] B. Hu, L. Fang, X. Cheng, and L. Yang, "In-vehicle caching (IV-cache) via dynamic distributed storage relay (D^2SR) in vehicular networks," *IEEE Trans. Veh. Technol.*, vol. 68, no. 1, pp. 843–855, Jan. 2019.

[21] T. Z. H. Ernest, A. S. Madhukumar, R. P. Sirigina, and A. K. Krishna, "A hybrid-duplex system with joint detection for interference-limited UAV communications," *IEEE Trans. Veh. Technol.*, vol. 68, no. 1, pp. 335–348, Jan. 2019.

[22] R. Narasimhan, "Finite-SNR diversity–multiplexing tradeoff for correlated rayleigh and Rician MIMO channels," *IEEE Trans. Inf. Theory*, vol. 52, no. 9, pp. 3965–3979, Sep. 2006.

[23] W.-Y. Shin, S.-Y. Chung, and Y. H. Lee, "Diversity–multiplexing tradeoff and outage performance for Rician MIMO channels," *IEEE Trans. Inf. Theory*, vol. 54, no. 3, pp. 1186–1196, Mar. 2008.

[24] T. Z. H. Ernest, A. S. Madhukumar, R. P. Sirigina, and A. K. Krishna, "Outage analysis and finite SNR diversity-multiplexing tradeoff of hybrid-duplex systems for aeronautical communications," *IEEE Trans. Wireless Commun.*, vol. 18, no. 4, pp. 2299–2313, Apr. 2019.

[25] F. Liang, C. Shen, W. Yu, and F. Wu, "Towards optimal power control via ensembling deep neural networks," *IEEE Trans. Commun.*, vol. 68, no. 3, pp. 1760–1776, Mar. 2020.

[26] T.-V. Nguyen, N.-N. Dao, V. D. Tuong, W. Noh, and S. Cho, "User-aware and flexible proactive caching using LSTM and ensemble learning in IoT-MEC networks," *IEEE Internet Things J.*, vol. 9, no. 5, pp. 3251–3269, Mar. 2022.

[27] T. Z. H. Ernest, A. S. Madhukumar, R. P. Sirigina, and A. K. Krishna, "Hybrid-duplex communications for multi-UAV networks: An outage probability analysis," *IEEE Commun. Lett.*, vol. 23, no. 10, pp. 1831–1835, Oct. 2019.

[28] Y. M. Saputra, D. T. Hoang, D. N. Nguyen, E. Dutkiewicz, D. Niyato, and D. I. Kim, "Distributed deep learning at the edge: A novel proactive and cooperative caching framework for mobile edge networks," *IEEE Wireless Commun. Lett.*, vol. 8, no. 4, pp. 1220–1223, Aug. 2019.

[29] L. Liang, J. Kim, S. C. Jha, K. Sivanesan, and G. Y. Li, "Spectrum and power allocation for vehicular communications with delayed CSI feedback," *IEEE Wireless Commun. Lett.*, vol. 6, no. 4, pp. 458–461, Aug. 2017.
[30] X. Li, L. Ma, Y. Xu, and R. Shankaran, "Resource allocation for D2D-based V2X communication with imperfect CSI," *IEEE Internet Things J.*, vol. 7, no. 4, pp. 3545–3558, Apr. 2020.
[31] C. Jiang, H. Zhang, Z. Han, Y. Ren, V. C. M. Leung, and L. Hanzo, "Information-sharing outage-probability analysis of vehicular networks," *IEEE Trans. Veh. Technol.*, vol. 65, no. 12, pp. 9479–9492, Dec. 2016.
[32] X. Ma, J. Zhao, Y. Wang, T. Zhang, and Z. Li, "A new approach to SINR-based reliability analysis of IEEE 802.11 broadcast ad hoc networks," *IEEE Commun. Lett.*, vol. 25, no. 2, pp. 651–655, Feb. 2021.
[33] Y. Lin, Z. Zhang, Y. Huang, J. Li, F. Shu, and L. Hanzo, "Heterogeneous user-centric cluster migration improves the connectivity-handover trade-off in vehicular networks," *IEEE Trans. Veh. Technol.*, vol. 69, no. 12, pp. 16027–16043, Dec. 2020.
[34] V. V. Chetlur and H. S. Dhillon, "Downlink coverage analysis for a finite 3-D wireless network of unmanned aerial vehicles," *IEEE Trans. Commun*, vol. 65, no. 10, pp. 4543–4558, Oct. 2017.
[35] X. Wang, H. Zhang, Y. Tian, and V. C. M. Leung, "Modeling and analysis of aerial base station-assisted cellular networks in finite areas under LoS and NLoS propagation," *IEEE Trans. Wireless Commun.*, vol. 17, no. 10, pp. 6985–7000, Oct. 2018.
[36] T. Kim, D. J. Love, and B. Clerckx, "Does frequent low resolution feedback outperform infrequent high resolution feedback for multiple antenna beamforming systems?" *IEEE Trans. Signal Process.*, vol. 59, no. 4, pp. 1654–1669, Apr. 2011.
[37] H. Kim, H. Yu, and Y. H. Lee, "Limited feedback for multicell zero-forcing coordinated beamforming in time-varying channels," *IEEE Trans. Veh. Technol.*, vol. 64, no. 6, pp. 2349–2360, Jun. 2015.
[38] M. Abramowitz and I. Stegun, *Handbook of Mathematical Functions With Formulas, Graphs, and Mathematical Tables* (Applied Mathematics Series 55), Washington, DC, USA: Nat. Bur. Stand., 1964.
[39] A. Bazzi, B. M. Masini, A. Zanella, and I. Thibault, "On the performance of IEEE 802.11p and LTE-V2V for the cooperative awareness of connected vehicles," *IEEE Trans. Veh. Technol.*, vol. 66, no. 11, pp. 10419–10432, Nov. 2017.
[40] A. Narayanan, S. Verma, E. Ramadan, P. Babaie, and Z.-L. Zhang, "DeepCache: A deep learning based framework for content caching," in *Proc. Workshop Netw. Meets AI ML*, 2018, pp. 48–53.
[41] R. Wang, Z. Kan, Y. Cui, D. Wu, and Y. Zhen, "Cooperative caching strategy with content request prediction in Internet of Vehicles," *IEEE Internet Things J.*, vol. 8, no. 11, pp. 8964–8975, Jun. 2021.
[42] L. Zhao, Y. Ran, H. Wang, J. Wang, and J. Luo, "Towards cooperative caching for vehicular networks with multi-level federated reinforcement learning," in *Proc. IEEE Int. Conf. Commun. (ICC)*, 2021, pp. 1–6.
[43] T. O'Shea and J. Hoydis, "An introduction to deep learning for the physical layer," *IEEE Trans. Cogn. Commun. Netw.*, vol. 3, no. 4, pp. 563–575, Dec. 2017.
[44] C. Zhong, M. C. Gursoy, and S. Velipasalar, "Deep reinforcement learning-based edge caching in wireless networks," *IEEE Trans. Cogn. Commun. Netw.*, vol. 6, no. 1, pp. 48–61, Mar. 2020.
[45] S. Müller, O. Atan, M. van der Schaar, and A. Klein, "Context-aware proactive content caching with service differentiation in wireless networks," *IEEE Trans. Wireless Commun.*, vol. 16, no. 2, pp. 1024–1036, Feb. 2017.
[46] N. B. Rached, A. Kammoun, M.-S. Alouini, and R. Tempone, "A unified moment-based approach for the evaluation of the outage probability with noise and interference," *IEEE Trans. Wireless Commun.*, vol. 16, no. 2, pp. 1012–1023, Feb. 2017.
[47] A. R. Heidarpour, G. K. Kurt, and M. Uysal, "Finite-SNR diversity-multiplexing tradeoff for network coded cooperative OFDMA systems," *IEEE Trans. Wireless Commun.*, vol. 16, no. 3, pp. 1385–1396, Mar. 2017.
[48] L. Zheng and D. N. C. Tse, "Diversity and multiplexing: A fundamental tradeoff in multiple-antenna channels," *IEEE Trans. Inf. Theory*, vol. 49, no. 5, pp. 1073–1096, May 2003.
[49] D. Liu and C. Yang, "Energy efficiency of downlink networks with caching at base stations," *IEEE J. Sel. Areas Commun.*, vol. 34, no. 4, pp. 907–922, Apr. 2016.
[50] Y. Li, S. Han, and C. Yang, "Multicell power control under rate constraints with deep learning," *IEEE Trans. Wireless Commun.*, vol. 20, no. 12, pp. 7813–7825, Dec. 2021.

TAN ZHENG HUI ERNEST received the B.Eng. (First-Class Hons.) and Ph.D. degrees in computer engineering from Nanyang Technological University in 2015 and 2020, respectively. He is currently a Development Scientist and a Technical Lead for Edge Computing with the Advanced Remanufacturing and Technology Centre (ARTC) under the Agency for Science, Technology and Research. Prior to this, he was a Research Engineer with Airbus Singapore Private Limited, with research activities focusing on the performance analysis of interference management strategies, nonorthogonal multiple access, and in-band full-duplex schemes, for fifth-generation (5G)-enabled aeronautical and unmanned aerial vehicle communications. His research activities at ARTC focuses on investigating 5G-and-beyond networks, machine-learning-driven wireless communications, learning-based edge caching strategies, and computation offloading protocols, for industrial Internet of Things networks.

A. S. MADHUKUMAR (Senior Member, IEEE) received the B.Tech. degree from the College of Engineering, Thiruvananthapuram, India, the M.Tech. degree from the Cochin University of Science and Technology, Cochin, India, and the Ph.D. degree from the Indian Institute of Technology Madras, Chennai, India.

He is currently an Associate Professor with the School of Computer Science and Engineering, Nanyang Technological University, Singapore. He was involved in communications and signal processing research with the Centre for Development of Advanced Computing, Government of India, and the Institute for Infocomm Research (previously known as the Centre for Wireless Communications), Singapore. His current research interests include heterogeneous networks, cooperative radio systems for mobile multihop networks, algorithms and architectures of cognitive radios, new modulation and multiple access schemes, and advanced signal processing algorithms for communication systems. He is involved in a number of funded research projects, organizing international conferences, and a permanent reviewer for many internationally reputed journals and conferences. He has authored or coauthored more than 300 referred international conference and journal papers.